American Mineralogist, Volume 97, pages 1320–1329, 2012

Thermal behavior of realgar As_4S_4, and of arsenolite As_2O_3 and non-stoichiometric As_8S_{8+x} crystals produced from As_4S_4 melt recrystallization

PAOLO BALLIRANO*

Dipartimento di Scienze della Terra, Sapienza Università di Roma, P.le Aldo Moro 5, I-00185 Roma, Italy

ABSTRACT

An in situ high-temperature X-ray powder diffraction study of the thermal behavior of realgar (α-As_4S_4) has been carried out. Data, measured in transmission geometry on a non-hermetically sealed capillary, indicate that the realgar → β-As_4S_4 phase transition starts at 558 K and is completed at 573 K due to kinetics. Melting starts at 578 K and is completed at 588 K. Thermal expansion of realgar is significant and fairly isotropic. In fact, the *a*- and *b*-parameters expand almost at the same rate, whereas the *c*-parameter is slightly softer against heating. Moreover, the β-angle contracts as temperature is raised. The geometry of the As_4S_4 molecule is largely independent from heating. The lengthening of a few As-S and As-As contacts above or near the sum of the As,S van der Waals radii represents the driving force of the phase transition. In addition, the thermal behavior of arsenolite As_2O_3 and non-stoichiometric As_8S_{8+x} crystals produced from As_4S_4 melt recrystallization has been investigated. Two members located along the β-As_4S_4-alacranite (As_8S_9) series joint were identified at RT: a term close to the β-As_4S_4 end-member (As_8S_{8+x}: x = ca. 0.1) and one term of approximate $As_8S_{8.3}$ composition. The thermal expansion of β-As_4S_4 is significantly anisotropic following the $\alpha_b > \alpha_a > \alpha_c$ relationship. This is clearly the result of the different packing scheme of the As_4S_4 cages in β-As_4S_4 with respect to realgar. The dependence of cell parameters and volume of $As_8S_{8.3}$ is more complicated. In fact, a strong discontinuity on the dependence of cell parameters and volume is observed in the 403–443 K thermal range, i.e., that at which $As_8S_{8.3}$ converts partly to realgar. A significant volume expansion is observed as a result of a change of composition to $As_8S_{8.7}$.

Keywords: Sulfides, realgar, alacranite, β-As_4S_4, arsenolite, high-temperature X-ray powder diffraction, Rietveld method

INTRODUCTION

Realgar is one of the four naturally occurring As_4S_4 polymorphs: α-As_4S_4 (realgar), β-As_4S_4, As_4S_4 (II), and pararealgar. A further high-pressure modification has been recently reported (Tuktabiev et al. 2009). The structure of realgar, first described by Ito et al. (1952), is characterized by the presence of covalently bonded As_4S_4 cages possessing an almost perfect point group $\bar{4}2m$ symmetry. Such cages are arranged in a zigzag way resulting in a layered structure with planes stacked along [010]. A description of the relationships existing among the various As_4S_4 polymorphs may be found in Ballirano and Maras (2006).

The most relevant and studied property of realgar is its light-induced alteration in ambient air (Clark 1970; Roberts et al. 1980; Douglass et al. 1992; Bonazzi et al. 1996; Kyono et al. 2005; Ballirano and Maras 2006; Bonazzi and Bindi 2008). Recent work agrees in identifying pararealgar and arsenolite (As_2O_3) as the final products of the process. The transformation proceeds via an intermediate term located along the β-As_4S_4-alacranite (As_8S_9) series joint (Ballirano and Maras 2006) due to the occurrence of the reaction $5As_4S_4 + 3O_2 \rightarrow 4As_4S_5 + 2As_2O_3$ proposed by Bindi et al. (2003). On the contrary, less effort has been devoted to the analysis of the thermal behavior of realgar. In fact, the only available information is that realgar converts to β-As_4S_4 over a composition-dependent temperature range of 512 to 535 K (Hall 1966; Roland 1972; Blachnik et al. 1980) and that melting of β-As_4S_4 occurs at 579(3) K (Roland 1966). However, no data about its thermal expansion, or its structure behavior, as a function of temperature are available in literature.

The present work aims to fill such a gap from laboratory parallel-beam X-ray powder diffraction data. Data have been collected in situ, in real-time and analyzed from room temperature (RT) up to melting. Moreover, the thermal behavior of the crystallization products of the corresponding quenched melt has been investigated.

EXPERIMENTAL METHODS

A fragment of a large crystal of realgar from Monte Sughereto, Latium, Italy, from the same batch of those previously investigated by Ballirano and Maras (2006), was crushed under ethanol in an agate mortar. The powder was loaded and packed in a 0.5 mm diameter quartz-glass capillary that was non-hermetically sealed. The capillary was fixed to a 1.0 mm diameter Al_2O_3 tube by means of a high-purity alumina ceramic (Resbond 989). The capillary/tube assembly was subsequently aligned onto a standard goniometer head and diffraction data were collected on a parallel-beam Bruker AXS D8 Advance, operating in transmission in θ-θ geometry, using Cu$K\alpha$ radiation. The instrument is fitted with a PSD VÅNTEC-1 detector set to a 6 °2θ aperture and with a prototype of capillary heating chamber (Ballirano and Melis 2007, 2009). Insertion of the capillary into the chamber prevented the powder from exposure to light.

A preliminary RT X-ray powder diffraction pattern confirmed the absence of alteration products of realgar as β-As_4S_4, pararealgar, and arsenolite. Non-ambient data were collected in the 10–140 °2θ angular range, step-size of 0.022 °2θ, with 3 s

* E-mail: paolo.ballirano@uniroma1.it

0003-004X/12/0809–1320$05.00/DOI: http://dx.doi.org/10.2138/am.2012.4114

of counting time, in the 303–503 K thermal range with temperature steps of 25 K and in the 508–598 K thermal range with temperature steps of 5 K. The capillary was subsequently quenched to RT and a new heating run was performed in the 303–603 K thermal range with temperature steps of 10 K.

Diffraction data of the heating run of realgar were evaluated with the GSAS suite of programs (Larson and Von Dreele 2000) coupled with the EXPGUI graphical user interface (Toby 2001). Peak shapes were modeled by a pseudo-Voigt function (Thompson et al. 1987) modified to incorporate asymmetry (Finger et al. 1994). Refined parameters were GV (tan θ-dependent Gaussian parameter), GW (angle-independent Gaussian term), LX (1/cosθ-dependent Lorentzian parameter), LY (tan θ-dependent Lorentzian parameter), and S/L, and H/L (asymmetry parameters, constrained to be equal in magnitude). However, a first series of refinements led to small values of LY that consistently approaching to zero. Therefore, to reduce the overall number of refined parameters and to improve the refinements stability, LY was reset to zero. Peak positions were corrected for sample displacement from the focusing circle. The peak cut-off was set to 0.03% of the peak maximum and background was fitted with a 36-terms Chebyshev polynomial of the first kind. An absorption parameter, including the contribution from the aluminum heating chamber windows, was refined at 303 K and kept fixed at that value for the whole data set.

Starting structural data of realgar were taken from Mullen and Nowacki (1972). A structure refined at a given temperature was used as input for the subsequent temperature. The following restraints were imposed, using a statistical weight of 10, on intramolecular bond distances and angles (expressed as pseudobonds): As-S 2.240(6) Å, As-As 2.570(3) Å, S-S (corresponding to S-As-S) 3.330(10) Å, As-As (corresponding to As-S-As) 3.460(11) Å, and As-S (corresponding to As-As-S) 3.673(9) Å. Such distances were taken from the reference RT refinement. The contribution of the restraints to χ^2 never exceeded 2.5% indicating a proper weighting scheme.

The evaluation of texture by means of a generalized spherical-harmonic description (Von Dreele 1997) confirmed the almost complete absence of preferred orientation over the full thermal range through observation of a very constant value, which was also close to one ($\bar{J}$ = 1.025) of the calculated texture indices *J*. The final structural data set was obtained by keeping the 8 spherical harmonics coefficients *l,m,n* fixed to the corresponding averaged values (2,0,$\bar{2}$ = 0.069; 2,0,0 = –0.263; 2,0,2 = –0.022; 4,0,$\bar{4}$ = 0.211; 4,0,$\bar{2}$ = –0.022; 4,0,0 = –0.190; 4,0,2 = –0.023; 4,0,4 = 0.118). A magnified view of the complete data set of the heating run of realgar, consisting of 29 diffraction patterns, is shown in Figure 1. Miscellaneous data of the Rietveld refinements are reported in Table 1. The CIF files[1] of the refined structures in the 303–578 K thermal range are deposited.

TABLE 1. Miscellaneous data of the Rietveld refinements of the heating run of realgar

χ^2	1.22–1.48
R_{wp} (%)	4.32–4.78
R_p (%)	3.41–3.74
R_{F2} (%)	7.79–17.96
DWd	1.55–1.70
Refined parameters*	73 / 95 / 70

Note: Statistic indicators as defined in Young (1993).
* Refers to refinement with: only realgar / realgar+β-As_4S_4 / only β-As_4S_4.

DISCUSSION

Thermal behavior of realgar

A visual inspection of the full data set of the heating run of realgar indicates the onset of a phase transition at 558 K. The newly formed phase is located along the β-As_4S_4-alacranite (As_8S_9) series join. According to the refined monoclinic cell parameters it could be hypothesized that the phase is reasonably close to the β-As_4S_4 composition as can be deduced from comparison with the RT cell data reported by Bonazzi et al. (2003a). In fact, the high-temperature (HT) *c*-parameter is very close to that reported at RT for several samples of stoichiometry near to the β-As_4S_4 end-member. Accordingly, the Rietveld refinement was carried out in space group *C*2/*c* using as starting structural data those of Burns and Percival (2001). The geometry of the As_4S_4 cage was restrained using the following intramolecular bond distances and angles: As-S 2.225(5) Å, As-As 2.600(5) Å, S-S (corresponding to S-As-S) 3.280(5) Å, As-As (corresponding to As-S-As) 3.455(5) Å. The realgar → β-As_4S_4 phase transition starts at 558 K and is completed at 573 K due to the kinetics of the process. Within this thermal range both phases coexist. This temperature is significantly higher than 536(3) K reported by Roland (1972) in the case of a stoichiometric As_4S_4 composition. Rietveld plots of the data collected at 573 K are reported in Figure 2. Melting starts at 578 K and is completed at 588 K. These temperatures compare favorably with the value of 579(2) K reported by Roland (1966). As far as the evolution of the cell parameters of realgar with temperature is concerned, they are listed in Table 2, whereas the relative expansion of cell parameters and volume is reported in Figure 3.

Thermal expansion of realgar is fairly isotropic. In fact, the *a*- and *c*-parameters expand almost at the same rate, whereas the *b*-parameter is slightly softer. Moreover, the β-angle contracts as temperature is raised. The dependence is quadric for all cell parameters. Small deviations from the regular behavior have been observed in the 558–568 K thermal range, possibly due to

[1] Deposit item AM-12-063, CIF. Deposit items are available two ways: For a paper copy contact the Business Office of the Mineralogical Society of America (see inside front cover of recent issue) for price information. For an electronic copy visit the MSA web site at http://www.minsocam.org, go to the *American Mineralogist* Contents, find the table of contents for the specific volume/issue wanted, and then click on the deposit link there.

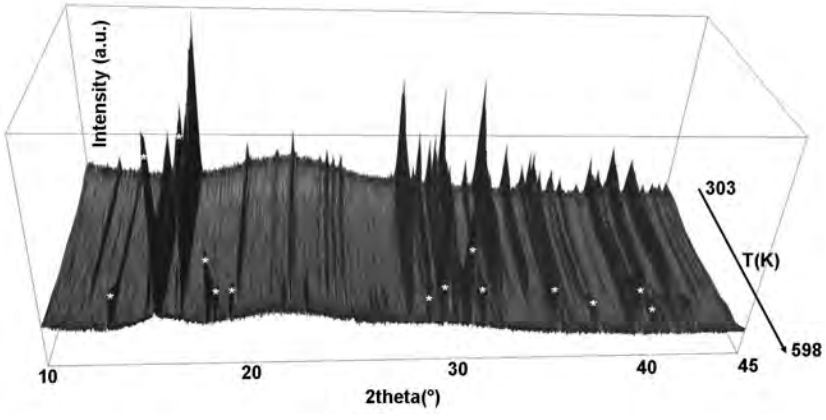

FIGURE 1. Magnified view (10–45 °2θ) of the full data set of the heating run of realgar. *: Main β-As_4S_4 reflections.

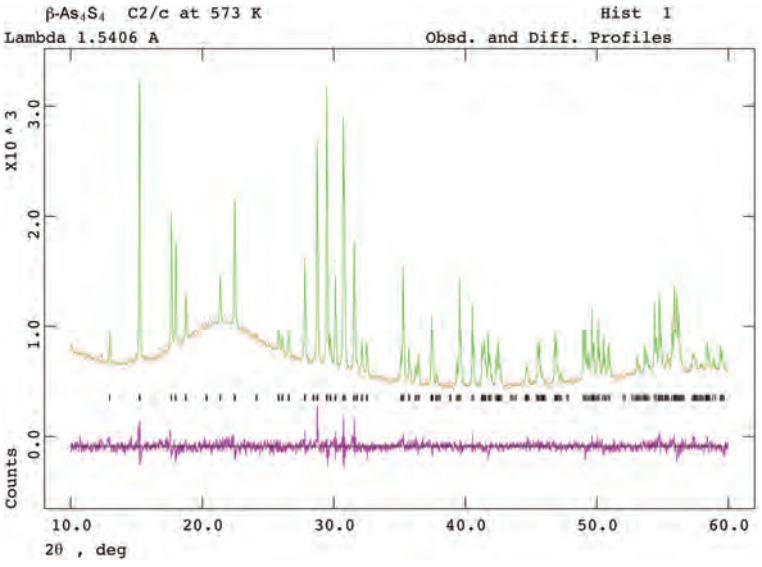

FIGURE 2. Magnified view (10–60 °2θ) of the Rietveld refinement of the diffraction pattern collected at 573 K. Dots = experimental; full line = calculated; below = difference. Vertical markers refer to the position of calculated Bragg reflections. (Color online.)

TABLE 2. Dependence of cell parameters and volume of realgar from temperature

T (K)	*a* (Å)	*b* (Å)	*c* (Å)	β (°)	*V* (Å³)
303	9.33037(13)	13.56790(14)	6.59251(7)	106.508(1)	800.155(15)
328	9.33880(10)	13.57931(14)	6.59866(8)	106.476(1)	802.443(16)
353	9.34680(11)	13.58948(15)	6.60436(8)	106.444(1)	804.562(17)
378	9.35542(11)	13.60050(16)	6.61034(8)	106.411(1)	806.822(18)
403	9.36391(13)	13.61168(18)	6.61630(9)	106.377(1)	809.09(2)
428	9.37236(14)	13.6212(2)	6.62224(10)	106.338(1)	811.32(2)
453	9.38121(15)	13.6338(2)	6.62859(10)	106.296(1)	813.75(2)
489	9.39030(15)	13.6451(2)	6.63520(11)	106.256(1)	816.19(3)
503	9.39910(17)	13.6570(2)	6.64164(12)	106.209(1)	818.66(3)
508	9.40071(19)	13.6590(3)	6.64287(13)	106.200(1)	819.10(3)
513	9.40324(18)	13.6615(3)	6.64448(13)	106.191(1)	819.71(3)
518	9.40477(18)	13.6638(3)	6.64564(13)	106.178(1)	820.18(3)
523	9.40710(18)	13.6667(3)	6.64722(13)	106.165(2)	820.81(3)
528	9.4089(2)	13.6688(3)	6.64863(14)	106.156(2)	821.30(3)
533	9.4106(2)	13.6710(3)	6.64978(14)	106.143(2)	821.78(3)
538	9.41276(19)	13.6743(3)	6.65168(14)	106.134(2)	822.44(3)
543	9.41502(19)	13.6769(3)	6.65258(14)	106.121(2)	822.99(3)
548	9.4172(2)	13.6794(3)	6.65429(15)	106.111(2)	823.55(3)
553	9.4188(2)	13.6822(3)	6.65599(17)	106.098(2)	824.12(4)
558	9.4200(3)	13.6852(5)	6.6578(2)	106.085(3)	824.69(5)
563	9.4206(7)	13.6863(9)	6.6598(5)	106.068(7)	825.12(8)

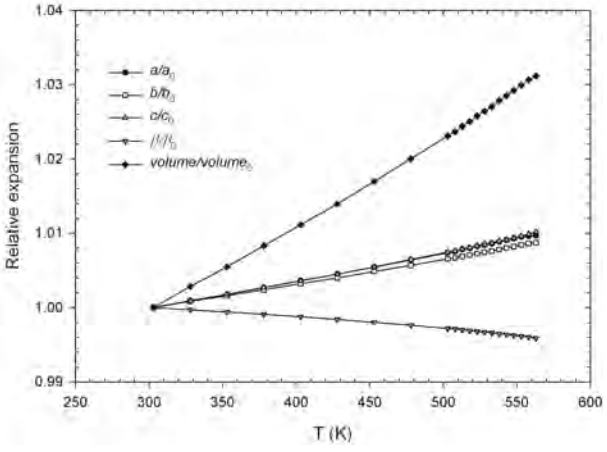

FIGURE 3. Relative expansion of cell parameters and volume of realgar with temperature.

correlations arising from the simultaneous occurrence of both realgar and β-As_4S_4. The volume thermal expansivity and the linear thermal expansion coefficients have been calculated applying the approach of Fei (1995) as described in Ballirano (2012) and Ballirano and Bosi (2012). Results of the fitting procedure are reported in Table 3. The thermal expansion of packed molecular realgar is significant and larger, as expected, than that of the ionic/covalently bonded sulfides listed by Skinner (1966). It is worth noting that the same cell volumes observed during the expansion caused by heating and those observed during the light induced alteration of realgar (Ballirano and Maras 2006) are obtained with different cell parameters. This indicates a significantly different level of microstrain developing during the two processes. In fact, Ballirano and Maras (2006) reported a large increase of strain during the light induced alteration of realgar, as determined from evaluation of the LY profile parameter. This behavior has been attributed to the need to preserve some structural coherency between at least two of the three simultaneously occurring sulfides (realgar, β-As_4S_4, pararealgar). On the contrary, in the case of the thermal expansion of realgar, LY was consistently close to zero indicating the absence of strain throughout the process (see Experimental methods). This is consistent with the observation that within the 558–568 K thermal range the volume of the two coexisting phases, realgar and β-As_4S_4, differs by ca. 0.9% only.

A detailed analysis of the realgar structure modification as a function of temperature has been performed. The As_4S_4 cage geometry has been found to be largely independent from heating. In particular bond distances were found to be constant at the 3σ level from 303 K to the transition temperature (As-As σ = ca. 0.001 Å; As-S σ = ca. 0.002 Å). Moreover, bond angles show limited, albeit regular, modifications as can be appreciated from Figure 4. The largest deformation is related to the increase of the

TABLE 3. Cell and volume thermal expansion coefficients a_0 and a_1 of realgar as measured in the heating run and in the re-heating experiment

		Heating run (T_r = 303 K)	Re-heating (T_r = 303 K)
a parameter	R^2	0.9997	0.9989
	a_0 (×10^{-4})	0.346(4)	0.344(5)
	a_1 (×10^{-8})	1.23(16)	1.0(3)
	a_{Tr}	9.33037(10)	9.3317(10)
b parameter	R^2	0.9998	0.9990
	a_0 (×10^{-4})	0.306(3)	0.331(5)
	a_1 (×10^{-8})	1.17(13)	0.7(3)
	b_{Tr}	13.56790(14)	13.5656(13)
c parameter	R^2	0.9996	0.9991
	a_0 (×10^{-4})	0.336(4)	0.354(5)
	a_1 (×10^{-8})	1.92(19)	1.3(3)
	c_{Tr}	6.59251(7)	6.5928(7)
β angle	R^2	0.9992	0.9966
	a_0 (×10^{-4})	–0.098(3)	–0.124(4)
	a_1 (×10^{-8})	–2.20(12)	–0.87(19)
	β_{Tr}	106.508(1)	106.504(9)
V	R^2	0.9998	0.9999
	a_0 (×10^{-4})	1.041(9)	1.098(5)
	a_1 (×10^{-8})	6.0(4)	3.9(3)
	V_{Tr}	800.165(15)	800.20(15)

Note: R^2 = determination coefficient.

As4-As1-S1 angle from ca. 99.1 to ca. 100.2°. All the remaining angles modify by a maximum of 0.5° within the analyzed thermal range. As expected, displacement parameters regularly increase with temperature.

To investigate the mechanism of the realgar → β-As_4S_4 phase transition a Hirshfeld surface of an As_4S_4 cage of realgar (Hirshfeld 1977) was calculated at each temperature from the correspondingly refined structural data. Figure 5 shows two such surfaces calculated, respectively, at 303 and 553 K, i.e., near the transition temperature. In particular, the contact distance d_{norm} was mapped onto the surface. Such distance combines both d_e (distance from a point on the surface to the nearest nucleus outside the surface) and d_i (distance from a point on the surface to the nearest nucleus inside the surface), each normalized by the van der Waals radius (r_i^{vdW}) for the particular atom involved in the close contact to the surface,

$$d_{\text{norm}} = \frac{d_i - r_i^{vdW}}{r_i^{vdW}} + \frac{d_e - r_i^{vdW}}{r_i^{vdW}}$$

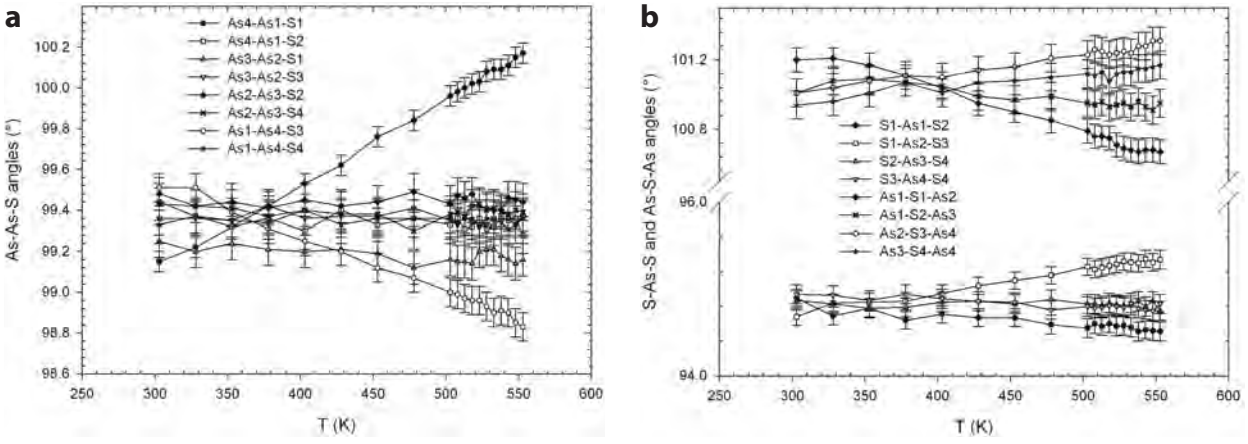

FIGURE 4. Evolution of bond angles of realgar with temperature: (**a**) As-As-S angles; (**b**) S-As-S and As-S-As angles.

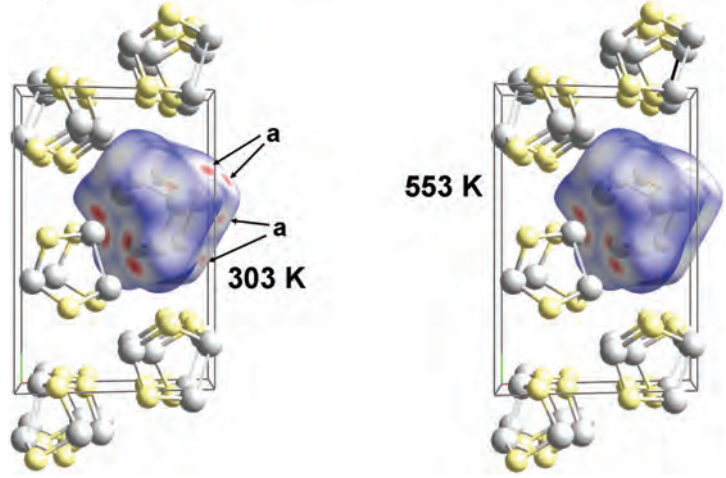

FIGURE 5. Hirshfeld surface of an As_4S_4 cage of realgar plotted at 303 and 553 K. The contact distance d_{norm} is mapped onto the surface on its natural range (i.e., from minimum to maximum) of –0.13 to 0.83. Color code goes from red (distances shorter than sum of van der Waals radii) through white to blue (distances longer than sum of van der Waals radii). Hirshfeld surfaces were calculated and plotted using CrystalExplorer 2.1 (Wolff et al. 2007). (Color online.)

(Spackman and Jayatilaka 2009). The contact distance d_{norm} is mapped on its natural range (i.e., from minimum to maximum) of –0.13 to 0.83. Therefore, the mapping color range spans from red (distances shorter than sum of van der Waals radii) through white to blue (distances longer than sum of van der Waals radii). Hirshfeld surfaces were calculated and plotted using CrystalExplorer 2.1 (Wolff et al. 2007). As can be seen, at 553 K the close contacts occurring at 303 K that are arrowed and labeled in the left panel of Figure 5, vanish causing the loss of the interaction that fasten together the A and B layers. As a further step, the evolution of the individual As-As (Fig. 6a) and As-S (Fig. 6b) intermolecular contacts has been analyzed the aim being to identify the driving force of the observed phase transition. Such transition results in a different packing scheme of the same type of As_4S_4 cages. In fact, in both minerals the cages are arranged in a zigzag fashion, resulting in a repeating corrugated layer structure. In the case of realgar, they are stacked along [010] with alternating A and B layers related by the *n* symmetry operator, whereas in β-As_4S_4 they are arranged following an …AA… sequence stacked along [110] (Ballirano and Maras 2006). Monitoring of the various intermolecular contact distances indicates that at the transition temperature, two of the seven As-S contacts occurring at RT (As2-S4 and As3-S3) exceed or equal the sum of the As,S van der Waals radii and three more (As1-As1, As1-As4, and As2-S1) are within 0.02 Å from the limit value. Therefore, it is expected that the weakening of those contacts should be the driving force of the transition. It is important to realize that, besides the relative independence of the geometry of the As_4S_4 cage from heating, the rate of expansion of the various intermolecular contacts is approximately the same, justifying the nearly isotropic thermal expansion of realgar.

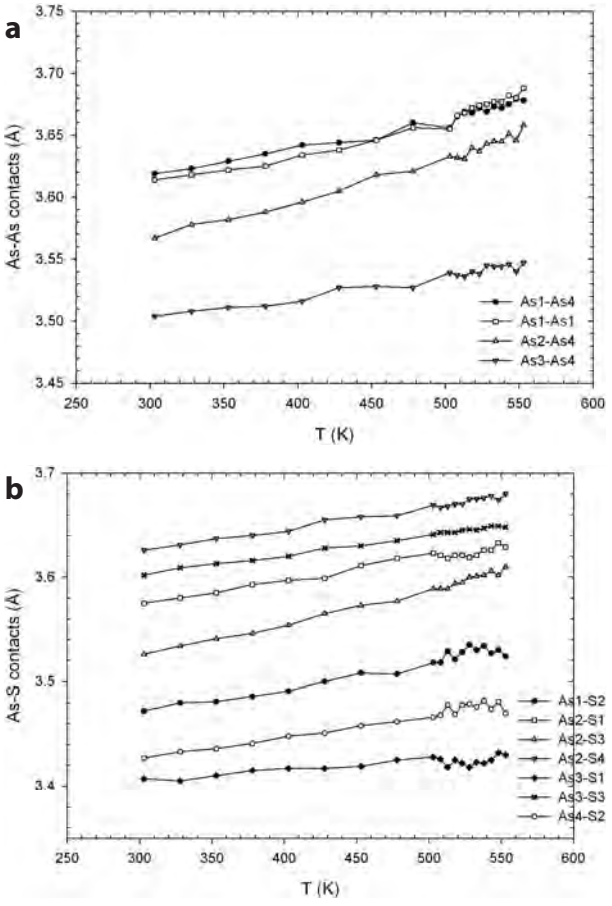

FIGURE 6. Evolution of intermolecular contacts: (**a**) As-As contacts; (**b**) As-S contacts.

As far as the thermal behavior of β-As_4S_4 is concerned, only minor structural differences were observed but whose quantitative relevance may be questionable as the analyzed thermal range spans over 30 K only, and therefore they will not be discussed.

Thermal behavior of the crystallization products of the quenched melt

The capillary was subsequently quenched at RT and a new heating run was performed. A magnified view of the complete data set, consisting of 31 diffraction patterns, is shown in Figure 7. Careful scrutiny of the RT data indicates the occurrence of four phases: realgar, arsenolite, and two distinct terms located along the β-As_4S_4-alacranite (As_8S_9) series joint (Popova et al. 1986; Bonazzi et al. 2003b). Intermediate terms of the series have been structurally described as arising from the simultaneous occurrence of β-As_4S_4 (space group $C2/c$) and As_8S_9 (space group $P2/c$) microdomains (Bonazzi et al. 2003a) whose distribution accounts for the gradual change of the translational lattice symmetry. Therefore, due to the complexity of the mixture, Rietveld refinements were performed with the aim being to perform quantitative phase analyses of the components of the mixture and to evaluate the evolution of cell parameters with temperature for each phase. Diffraction data were evaluated using TOPAS v4.2 (Bruker AXS 2009). This program implements the fundamental parameters approach, FPA (Cheary and Coelho 1992). FPA is a convolution approach in which the peak-shape is synthesized from a priori known features of the diffractometer and the microstructural features of the specimen. This approach has been demonstrated to improve the stability and the quality of the refinement.

Refined RT cell parameters of the two members of As_8S_{8+x} composition pointed to the occurrence of a term close to the β-As_4S_4 end-member (As_8S_{8+x}: x = ca. 0.1), hereinafter referred to as β-As_4S_4, and one term of approximate As_8S_{8+x} (x = ca. 0.3–0.4) composition, hereinafter referred to as As_8S_{8+x}, as derived from the regression line V (Å^3) = 801(2) + 1.04(5) [%As_4S_5] of Bonazzi et al. (2003a). Moreover, the latter has a composition reasonably close to that reported for sample ALA15, investigated from X-ray single-crystal diffraction data by those authors, whose structural data were used as input for the Rietveld refinements. Starting structural data of realgar were those obtained at 303 K in the present work; those of arsenolite and β-As_4S_4 (approximating the $As_8S_{8.1}$ structure) were taken from Ballirano and Maras (2002) and Burns and Percival (2001), respectively. The only refined structural parameter, apart from the cell dimensions, was k (Bonazzi et al. 2003a), the variable controlling the fraction of As_4S_5 cages occurring within the structure of As_8S_{8+x}. To reduce correlations among parameters, the absorption parameter was refined at

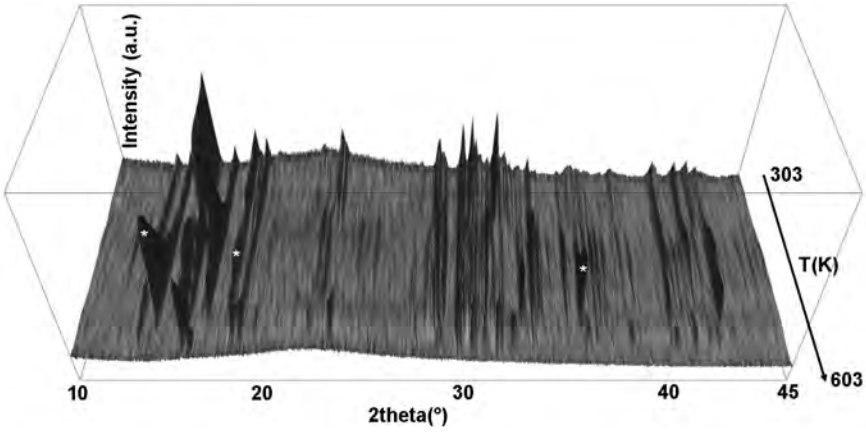

FIGURE 7. Magnified view (10–45°2θ) of the full data set of the heating run of the quenched melt. * Main arsenolite reflections.

each temperature compensating the increase of the displacement parameters with increasing temperature. The variation of the composition of the mixture with temperature is graphically displayed in Figure 8.

Quenching at RT of the melt produced during the first heating run resulted in 69.3(7) wt% of As_8S_{8+x}, 14.9(6) wt% of β-As_4S_4, 12.1(4) wt% of realgar, and 3.7(2) wt% of arsenolite. The relative abundance of the four phases remained substantially unchanged up to 403 K. At that temperature both β-As_4S_4 and As_8S_{8+x} started to convert to realgar. The maximum content of realgar occurred at 443 K [47.0(13) wt%]. In the 443–533 K thermal range the β-As_4S_4 content was nearly detectable (2–3 wt%), whereas that of arsenolite increased significantly. Moreover, realgar content decreased, whereas that of As_8S_{8+x} was substantially unchanged. At 543 K, β-As_4S_4 started to increase at the expenses of the remaining three phases. At 553 K only β-As_4S_4 and As_8S_{8+x} were still present and at 573 K only β-As_4S_4 was observed. Moreover, at 573 K the simultaneous increase of the background signaled the starting of the melting process. Above this temperature the background remained substantially unchanged. At 583 K the very partial crystallization of a phase was signaled by the occurrence of sharp reflections at *d*-spacings of ca. 5.67, 4.91, 2.96, and 2.84 Å. A subsequent test reproducing the heating cycles does not led to the crystallization of such phase. Therefore, due to the rapid change of the chemistry occurring in the open system represented by the capillary, no speculations about its identification can be safely made.

Melting was completed at 593 K. Comparison of the diffraction patterns of the melts obtained during the two experiments (Fig. 9) shows relevant differences. In fact, the diffraction pattern of the melt obtained from heating of realgar shows two main bands occurring at Q momentum transfer values [defined as $Q = (4\pi\sin\theta)/\lambda$] of ca. 1.1 and 1.5 $Å^{-1}$, a shoulder at 2.0 $Å^{-1}$, and two broad bands at 3.8 and 5.2 $Å^{-1}$. As can be seen from Figure 9, the contribution to the diffraction pattern of the SiO_2-glass of the capillary is located at Q of ca. 1.75 $Å^{-1}$. By contrast, the diffraction pattern of the melt from the second heating run lacks the strong band at Q of 1.1 $Å^{-1}$ and shows two less defined broad bands, as compared to the first heating run, in the 3.5 < Q

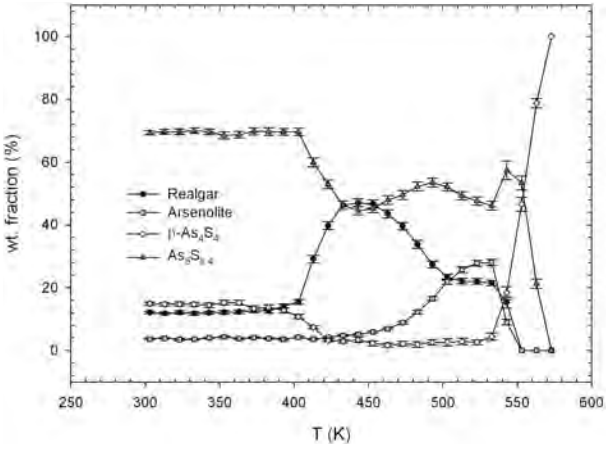

FIGURE 8. Dependence of the composition of the mixture from temperature.

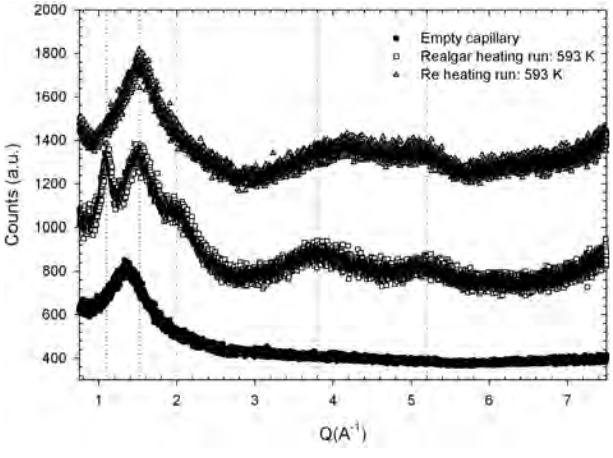

FIGURE 9. Diffraction patterns of the melts obtained during the two heating runs. For comparison purposes the diffraction pattern of an empty SiO_2-glass capillary is also reported.

< 5.5 Å^{-1} range. It is worth noting that the first strong band at Q of 1.1 Å^{-1} correspond to a *d*-spacing of ca. 5.7 Å, a value close to the distance measured at RT between centroids of the closest neighboring As_4S_4 cages in both crystalline realgar (Kyono et al. 2005) and β-As_4S_4, as recalculated from the structural data of Burns and Percival (2001).

The dependence of cell parameters and volume from temperature has been evaluated for all four phases occurring at RT. The volume thermal expansivity and the linear thermal expansion coefficients have been calculated following the same procedure above described for realgar. The evolution of cell parameters and volume of realgar with temperature is fully consistent with that observed during the first heating run. Cell and volume thermal expansion coefficients a_0 and a_1 are reported in Table 3. No significant differences are observed between the two data sets.

Cell and volume thermal expansion coefficients a_0 and a_1 of β-As_4S_4 are reported in Table 4. Due to the very small amount of β-As_4S_4, within the 423–533 K thermal range refined cell parameters were found to oscillate wildly. Therefore, in the final refinements they were kept fixed to the corresponding values obtained by interpolation, using a quadric dependence from *T*, of the cell parameters determined outside that thermal range. Comparison between the cell parameters of β-As_4S_4 obtained in the two experiments (direct conversion of realgar and crystallization from melt) indicates that they are similar albeit non-identical. This could provide an indication of a slightly different As_8S_{8+x} composition and/or a different amount of microstrain. In effect, the volume at the same temperature of β-As_4S_4 obtained from direct conversion of realgar (Fig. 10) is consistently ca. 4 Å^3 smaller than that obtained from crystallization of the melt, whose composition has been estimated to be of $As_8S_{8.1}$. According to the fact that a volumetric increase of ca. 1 Å^3 corresponds to an increase of x = ca. 0.02, as resulting from the regression line of Bonazzi et al. (2003a), the composition of As_8S_{8+x} obtained from direct conversion of realgar is close to that of the β-As_4S_4 end-member. This fact indicates that the realgar → β-As_4S_4 phase transition occurs with the persistence of the As:S = 1:1 ratio, at least up to melting, as confirmed by the absence of arsenolite during the heating run of realgar. Differently from realgar, thermal expansion of β-As_4S_4 is significantly anisotropic following the $\alpha_b > \alpha_a > \alpha_c$ relationship. This is clearly the result of the different packing scheme of the As_4S_4 cages as compared to realgar. In fact, there is a lack of distances shorter than the sum of van der Waals radii along the *b*-axis as can be seen from the Hirshfeld surface calculated at RT from the structural data of Porter and Sheldrick (1972) with the contact distance d_{norm} mapped onto the surface (Fig. 11).

The dependence of cell parameters and volume of As_8S_{8+x} from temperature is reported in Figure 12. By comparison with the cell data of the sample ALA15, of $As_8S_{8.4}$ composition (Bonazzi et al. 2003a), it is clear that the present As_8S_{8+x} sample has sulfur content slightly smaller. Furthermore, it should be noted that the composition of ALA15 was of $As_8S_{8.42}$ from X-ray single-crystal refinement and $As_8S_{8.46}$ from unit-cell volume evaluation. In effect, the same overestimation of the sulfur content has been observed in the present work as the composition of $As_8S_{8.3}$ has been obtained from the site occupancy factor (sof) refinement of the various sites, following the same procedure depicted in Bonazzi et al. (2003a) (Fig. 13) as compared to $As_8S_{8.4}$ obtained from unit-cell volume evaluation. A strong discontinuity on the dependence of cell parameters and volume is observed in the 403–443 K thermal range, i.e., that at which $As_8S_{8.3}$ partly converts to realgar. In fact, a significant volume expansion is observed as a result

TABLE 4. Cell and volume thermal expansion coefficients a_0 and a_1 of β-As_4S_4

	R^2	β-As_4S_4 (T_r = 303 K)		
		a_0 (×10^{-4})	a_1 (×10^{-8})	
a parameter	0.9989	0.428(11)	2.7(5)	a_{Tr} = 9.9768(18)
b parameter	0.9974	0.703(19)	–4.5(8)	b_{Tr} = 9.3196(18)
c parameter	0.9961	0.061(17)	12.3(7)	c_{Tr} = 8.8838(13)
β angle	0.8902	–0.004(9)	–1.3(4)	β_{Tr} = 102.601(13)
V	0.9989	1.19(3)	11.8(14)	V_{Tr} = 806.1(2)

Note: R^2 = determination coefficient.

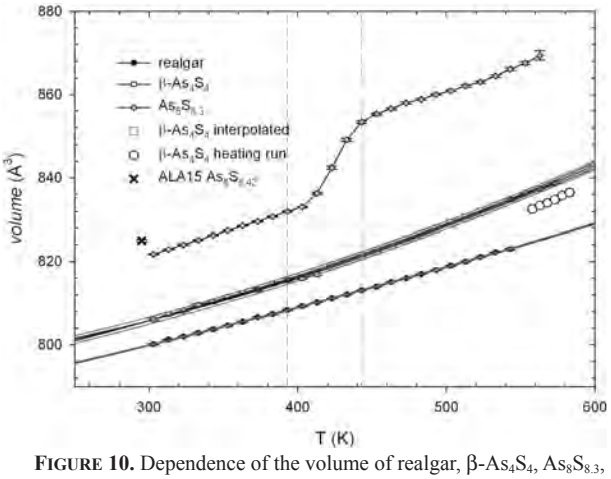

FIGURE 10. Dependence of the volume of realgar, β-As_4S_4, $As_8S_{8.3}$, and arsenolite from temperature. Confidence (95% level), and prediction intervals are reported as full, dotted, and short dash lines, respectively.

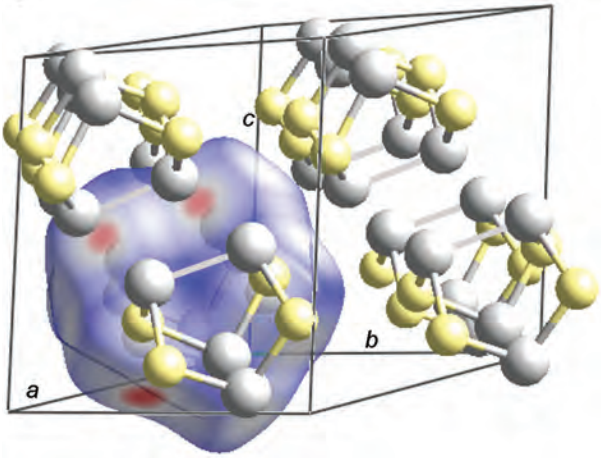

FIGURE 11. Hirshfeld surface of an As_4S_4 cage of β-As_4S_4 plotted at RT. The contact distance d_{norm} is mapped onto the surface. Structural data taken from Porter and Sheldrick (1972). (Color online.)

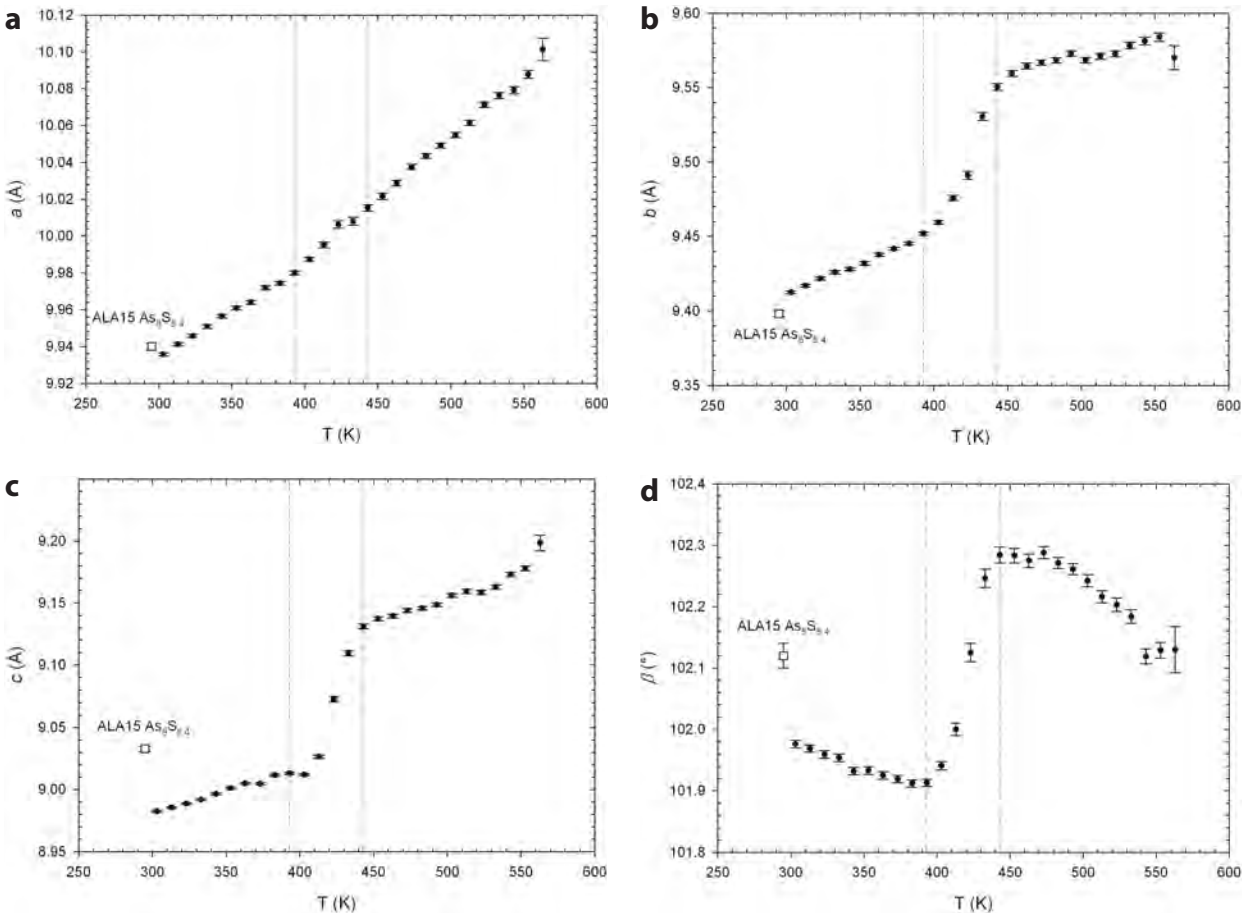

FIGURE 12. Evolution of cell parameters and volume of $As_8S_{8.3}$ with temperature: (**a**) *a*-parameter; (**b**) *b*-parameter; (**c**) *c*-parameter; (**d**) β-angle. Reference data of sample ALA15, of $As_8S_{8.4}$ composition (Bonazzi et al. 2003a), have been reported for comparison.

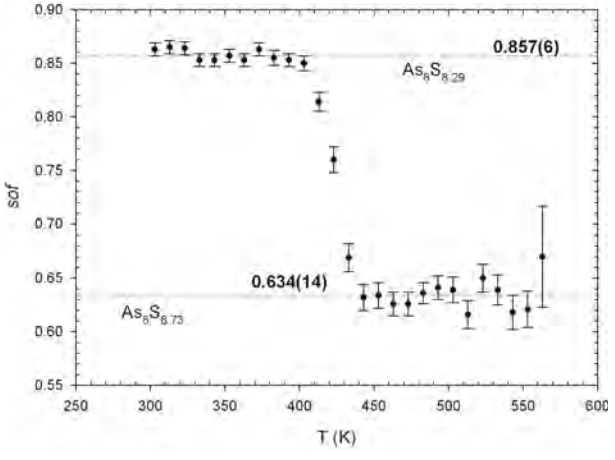

FIGURE 13. Dependence of the site occupancy factor (sof) of the various sites of $As_8S_{8.3}$ [constrained as in Bonazzi et al. (2003a)] from temperature.

of a change of composition to $As_8S_{8.7}$ as determined from sof refinements. Interpolation of the volume data of $As_8S_{8.3}$ at 443 K indicates an expansion of ca. 18 Å^3 fully consistent with the $As_8S_{8.7}$ composition obtained from sof refinements. Therefore, it may be reasonably hypothesized that conversion of $As_8S_{8.3}$ to realgar occurs within the microdomains with β-As_4S_4 structure, whereas the relative volumetric increase of microdomains with As_8S_9 structure accordingly modifies the overall composition of the As_8S_{8+x} phase. Furthermore, this fact confirms the correctness of the structure description of the intermediate terms of the β-As_4S_4-alacranite (As_8S_9) series proposed by Bonazzi et al. (2003a) on the basis of the coexistence of disordered As_8S_8 and As_8S_9 microdomains. Above 443 K the $As_8S_{8.7}$ composition remains unchanged.

Comparison between the relative expansion of cell parameters and volume for both β-As_4S_4 and the As_8S_{8+x} phase is reported in Figure 14. Data evaluation is rendered difficult by the absence of experimental data in the 423–533 K thermal range for β-As_4S_4 and the change in composition of the As_8S_{8+x} phase occurring in the 403–443 K thermal range. The relative

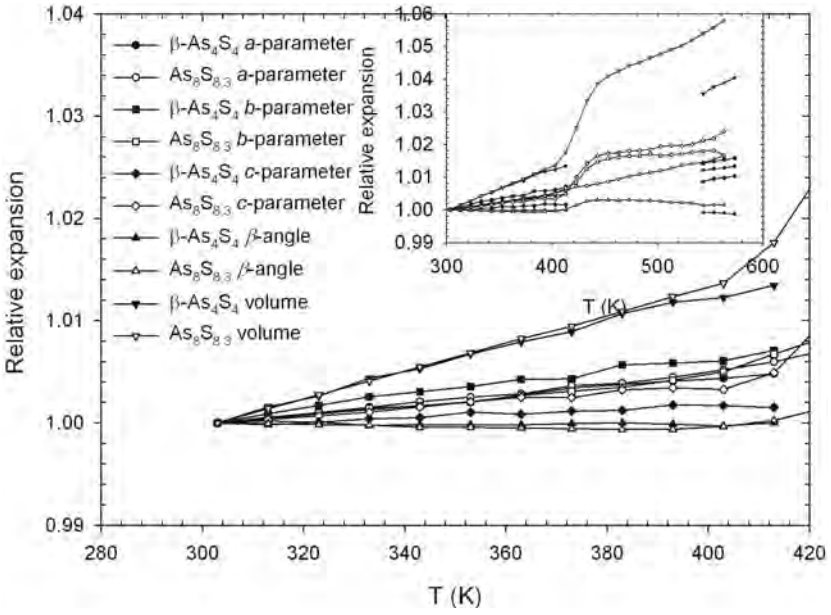

FIGURE 14. Relative expansion of cell parameters and volume of realgar with temperature in the 303–413 K thermal range. Inset full analyzed thermal range.

TABLE 5. Dependence of the *a*-parameter of arsenolite from temperature

T (K)	*a* (Å)	*T* (K)	*a* (Å)
303	11.0770(8)	433	11.1403(5)
313	11.0849(9)	443	11.1441(4)
323	11.0895(9)	453	11.1493(3)
333	11.0938(9)	463	11.1549(3)
343	11.0977 (8)	473	11.16022(19)
353	11.1046(8)	483	11.16560(13)
363	11.1070(8)	493	11.17138(10)
373	11.1106(8)	503	11.17686(8)
383	11.1163(8)	513	11.18217(7)
393	11.1207(8)	523	11.18777(7)
403	11.1250(6)	533	11.19372(7)
413	11.1304(6)	543	11.1983(3)
423	11.1341(6)		

TABLE 6. Cell expansion coefficients a_0 and a_1 of arsenolite

		Arsenolite (T_r = 303 K)
a parameter	R^2	0.9983
	a_0 (×10^{-4})	0.427(8)
	a_1 (×10^{-8})	1.1(4)
	a_{Tr}	11.0770(8)

Note: R^2 = determination coefficient.

expansion of both phases is not identical as in the 303–413 K thermal range As_8S_{8+x} follows the $\alpha_b = \alpha_a > \alpha_c$ relationship instead of $\alpha_b > \alpha_a > \alpha_c$ shown by β-As_4S_4.

Finally, the dependence of the *a*-parameter and the cell thermal expansion coefficients a_0 and a_1 of arsenolite are reported in Table 5 and 6, respectively.

ACKNOWLEDGMENTS

This work was funded by Sapienza Università di Roma. I am grateful to A. Kyoto and an anonymous reviewer for their critical reading of the manuscript.

REFERENCES CITED

Ballirano, P. (2012) The thermal behavior of liottite. Physics and Chemistry of Minerals, 39, 115–121.

Ballirano, P. and Bosi, F. (2012) Thermal behavior of afghanite, an ABABACAC member of the cancrinite group. American Mineralogist, 97, 630–640.

Ballirano, P. and Maras, A. (2002) Refinement of the crystal structure of arsenolite, As_2O_3. Zeitschrift für Kristallographie. New Crystal Structures, 217, 177–178.

——— (2006) In-situ X-ray transmission powder diffraction study of the light induced alteration of realgar (α-As_4S_4). European Journal of Mineralogy, 18, 589–599.

Ballirano, P. and Melis, E. (2007) Thermal behavior of β-anhydrite $CaSO_4$ to 1263 K. Physics and Chemistry of Minerals, 34, 699–704.

——— (2009) Thermal behavior and kinetics of dehydration of gypsum in air from in situ real-time laboratory parallel-beam X-ray powder diffraction. Physics and Chemistry of Minerals, 36, 391–402.

Bindi, L., Popova, V., and Bonazzi, P. (2003) Uzonite, As_4S_5, from the type locality: single-crystal X-ray study and effects of exposure to light. Canadian Mineralogist, 41, 1463–1468.

Blachnik, R., Hoppe, A., and Wickel, U. (1980) Die Systeme Arsen-Schwefel und Arsen-Selen und die thermodynamischen Daten ihrer Verbindungen. Zeitschrift für Anorganische und Allgemeine Chemie, 463, 78–90.

Bonazzi, P. and Bindi, L. (2008) A crystallographic review of arsenic sulfides: Effects of chemical variations and changes induced by exposure to light. Zeitschrift für Kristallographie, 223, 132–147.

Bonazzi, P., Menchetti, S., Pratesi, G., Muniz-Miranda, M., and Sbrana, G. (1996) Light-induced variations in realgar and β-As_4S_4: X-ray diffraction and Raman studies. American Mineralogist, 81, 874–880.

Bonazzi, P., Bindi, L., Olmi, F., and Menchetti, S. (2003a) How many alacranites do exists? A structural study of non-stoichiometric As_8S_{9-x} crystals. European Journal of Mineralogy, 15, 283–288.

Bonazzi, P., Bindi, L., Popova, V., Pratesi, G., and Menchetti, S. (2003b) Alacranite, As_8S_9: structural study of the holotype and re-assignment of the original chemical formula. American Mineralogist, 88, 1796–1800.

Bruker AXS (2009) Topas V4.2: General profile and structure analysis software for powder diffraction data. Bruker AXS, Karlsruhe, Germany.

Burns, P.C. and Percival, J.B. (2001) Alacranite, As_8S_4: A new occurrence, new formula, and determination of the crystal structure. Canadian Mineralogist, 39, 809–818.

Cheary, R.W. and Coelho, A. (1992) A fundamental parameters approach to X-ray line-profile fitting. Journal of Applied Crystallography, 25, 109–121.

Clark, A.H. (1970) Alpha-arsenic sulphide, from Mina Alacran, Pampa Larga, Chile. American Mineralogist, 55, 1338–1344.

Douglass, D.L., Shing, C., and Wang, G. (1992) The light-induced alteration of realgar to pararealgar. American Mineralogist, 77, 1266–1274.

Fei, Y. (1995) Thermal expansion. In J.A. Ahrens, Ed., A handbook of physical constants, mineral physics and crystallography. AGU Reference Shelf 2, 29–44.

Finger, L.W., Cox, D.E., and Jephcoat, A.P. (1994) A correction for powder diffraction peak asymmetry due to axial divergence. Journal of Applied Crystal-

lography, 27, 892–900.
Hall, H.T. (1966) The system Ag-Sb-S, Ag-As-S, and Ag-Bi-S: Phase relations and mineralogical significance. Ph.D. thesis, Brown University, Providence, Rhode Island, 172 pp.
Hirshfeld, F.L. (1977) Bonded-atom fragments for describing molecular charge densities. Theoretica Chimica Acta, 44, 129–138.
Ito, T., Morimoto, N., and Sadanaga, R. (1952) The crystal structure of realgar. Acta Crystallographica, 5, 775–782.
Kyono, A., Kimata, M., and Hatta, T. (2005) Light-induced degradation dynamics in realgar: in situ structural investigation using single-crystal X-ray diffraction study and X-ray photoelectron spectroscopy. American Mineralogist, 90, 1563–1570.
Larson, A.C. and Von Dreele, R.B. (2000) General Structure Analysis System (GSAS). Los Alamos National Laboratory Report LAUR 86-748.
Mullen, D.J.E. and Nowacki, W. (1972) Refinement of the crystal structures of realgar, AsS and orpiment, As_2S_3. Zeitschrift für Kristallographie, 136, 48–65.
Popova, V.I., Popov, V.A., Clark, A., Polyakov, V.O., and Borisovski, S.E. (1986) Alacranite As_8S_9; A new mineral. Proceedings of the Russian Mineralogical Society (ZVMO), 15, 360–368 (in Russian).
Porter, E.J. and Sheldrick, G.M. (1972) Crystal structure of a new crystalline modification of tetra-arsenic tetrasulphide (2,4,6,8-tetrathia-1,3,5,7-tetra-arsatricyclo[3,3,0,$0^{3,7}$]-octane. Journal of the Chemical Society, Dalton Transactions, 13, 1347–1349.
Roberts, A.C., Ansell, H.G., and Bonardi, M. (1980) Pararealgar, a new polymorph of AsS from British Columbia. Canadian Mineralogist, 18, 525–527.
Roland, G.W. (1966) Phase relations and geological application of the system Ag-As-S, 191 p. Ph.D. thesis, Lehigh University, Bethlehem, Pennsylvania.
——— (1972) Concerning the α-AsS ↔ realgar inversion. Canadian Mineralogist, 11, 520–525.
Skinner, B.J. (1966) Thermal expansion. In S.P. Clark, Jr., Ed., Handbook of Physical Constants, p. 75–95. Geological Society of America Memoirs, Boulder, Colorado.
Spackman, M.A. and Jayatilaka, D. (2009) Hirshfeld surface analysis. CrystEngComm, 11, 19–32.
Thompson, P., Cox, D.E., and Hastings, J.B. (1987) Rietveld refinement of Debye-Scherrer synchrotron X-ray data from Al_2O_3. Journal of Applied Crystallography, 20, 79–83.
Toby, B.H. (2001) EXPGUI, a graphical user interface for GSAS. Journal of Applied Crystallography, 34, 210–213.
Tuktabiev, M.A., Popova, S.V., Brazhkin, V.V., Lyapin, A.G., and Katayama, Y. (2009) Compressibility and polymorphism of α-As_4S_4 realgar under high pressure. Journal of Physics; Condensed Matter, 23, 385401.
Von Dreele, R.B. (1997) Quantitative texture analysis by Rietveld refinement. Journal of Applied Crystallography, 30, 517–525.
Wolff, S.K., Grimwood, D.J., McKinnon, J.J., Jayatilaka, D., and Spackman, M.A. (2007) CrystalExplorer 2.1. University of Western Australia.
Young, R.A. (1993) Introduction to the Rietveld method. In R.A. Young, Ed., The Rietveld Method, p. 1–38. Oxford, U.K.

Manuscript received January 23, 2012
Manuscript accepted May 18, 2012
Manuscript handled by Jennifer Kung